Proc. Natl. Acad. Sci. USA
Vol. 93, pp. 1913–1917, March 1996
Biophysics

Detection of sub-8-nm movements of kinesin by high-resolution optical-trap microscopy

CHRIS M. COPPIN*†, JEFFREY T. FINER‡, JAMES A. SPUDICH‡, AND RONALD D. VALE*§

*Department of Pharmacology and §Howard Hughes Medical Institute, University of California, San Francisco, CA 94143; and ‡Departments of Biochemistry and Developmental Biology, Beckman Center, Stanford University School of Medicine, Stanford, CA 94305

Contributed by James A. Spudich, November 20, 1995

ABSTRACT **Kinesin is a molecular motor that transports organelles along microtubules. This enzyme has two identical 7-nm-long motor domains, which it uses to move between consecutive tubulin binding sites spaced 8 nm apart along a microtubular protofilament. The molecular mechanism of this movement, which remains to be elucidated, may be common to all families of motor proteins. In this study, a high-resolution optical-trap microscope was used to measure directly the magnitude of abrupt displacements produced by a single kinesin molecule transporting a microscopic bead. The distribution of magnitudes reveals that kinesin not only undergoes discrete 8-nm movements, in agreement with previous work [Svoboda, K., Schmidt, C. F., Schnapp, B. J. & Block, S.M. (1993) *Nature (London)* 365, 721–727], but also frequently exhibits smaller movements of about 5 nm. A possible explanation for these unexpected smaller movements is that kinesin's movement from one dimer to the next along a protofilament involves at least two distinct events in the mechanical cycle.**

Kinesin is a motor that transports organelles toward the plus end of microtubules (1, 2). This protein, which bears some structural resemblance to the actin-based motor myosin, is a dimer of two identical 110-kDa subunits containing a pair of 7-nm force-generating heads (motor domains) (3), a 70-nm α-helical coiled-coil stalk, and small C-terminal domains that can associate with a pair of light chains (4). Unlike myosin, kinesin is a highly processive motor, meaning that a single kinesin molecule can travel for long distances (>1 μm) without loosing hold of the microtubule (5–8). Hence, it is possible to monitor repeating chemomechanical cycles as the motor travels along the microtubule.

The mechanical cycle of a single kinesin molecule transporting a microscopic bead in the force field of a laser trap can now be studied by high-resolution optical microscopy. This approach permits the measurement of nanometer displacements and piconewton forces on a millisecond time scale (9–12). In a previous study, Svoboda *et al*. (9) analyzed data obtained with an optical-trapping interferometer and found that kinesin pauses at 8-nm intervals, which corresponds to the distance between consecutive tubulin dimers along a microtubular protofilament. Since few abrupt movements were resolvable, that study made use of a frequency analysis of the distribution of point-to-point distance between all pairs of recorded kinesin positions to infer that kinesin moves predominantly in 8-nm steps.

In this study, the intention was to measure directly the abrupt displacements of a microscopic bead being pulled along a microtubule by a single kinesin molecule. This was achieved by using an optical microscope equipped with a quadrant photodiode detector capable of tracking the position of the bead with nanometer accuracy on a millisecond time scale (10). An optical trap was used to exert a backward load on the motor and to reduce the brownian motion of the bead. Due to the high signal-to-noise ratio in the positional data, more than half of the displacements produced by the motor could be identified as abrupt movements and measured. The distribution of magnitudes reveals that kinesin generates at least two types of movements: ≈8 nm [consistent with the report of Svoboda *et al*. (9) and with the microtubular lattice periodicity] and ≈5 nm, which was unexpected. The finding of displacements that are smaller than the intertubulin dimer spacing along a protofilament provides new clues on how kinesin moves along a microtubule.

MATERIALS AND METHODS

Sample Preparation and Assay. Casein (Sigma) in 10 mM Tris·HCl, pH 7.8/150 mM NaCl, was stirred overnight at 4°C, then centrifuged (20 min at $2 \times 10^5 \times g$), and the clear middle layer was recovered. Aliquots were stored at −20°C and centrifuged to clarity immediately before use. Polycarboxylated latex beads (0.931 ± 0.004 μm in diameter) (Polysciences) were washed with BRB80 (80 mM Pipes/1 mM $MgCl_2$/1 mM EGTA, pH 6.8), incubated in casein (3 mg/ml) for 1 hr at 4°C, and then washed twice with BRB80. Approximately 4×10^6 beads were incubated with ≈5 pg (8×10^6 molecules) of kinesin [purified according to Schnapp and Reese (13)] in BRB80 for >10 min at 0°C, yielding a nominal mean surface density of ≈two kinesins per bead. Beads were then suspended at ≈10^4 beads per μl in assay buffer [BRB80 with 20 μM ATP/10 mM glucose/glucose oxidase (30 μg/ml)/catalase (0.1 mg/ml)/0.2% 2-mercaptoethanol/1 mM dithiothreitol/1 mM phosphocreatine/creatine phosphokinase (0.1 mg/ml)/casein (≈0.3 mg/ml)]. Axonemes and repolymerized microtubules can be used interchangeably as a motility substrate in this kind of assay (7), but axonemes offer the advantage of being more rigid, binding more tightly to the glass, and keeping the bead farther away from the glass surface by virtue of their greater diameter. Sea urchin sperm axonemes (14) were fluorescently labeled <48 hr before use with 2 μM 5-(and-6)-carboxytetramethylrhodamine succinimidyl ester (Molecular Probes) in BRB80 (pH adjusted to 8.0) for 1 hr at 25°C, washed twice by sedimentation and resuspension in BRB80, and stored at 4°C. Immediately before an experiment, fluorescent axonemes were adsorbed to a final density of ≈300 axonemes per mm^2 on the inner surface of a flow chamber consisting of a glass slide and coverslip separated by two strips of adhesive tape. Microscopy, instrument calibrations, and data recording were performed according to Finer *et al*. (10). The analog positional signal bandwidth was 110 Hz, and the sampling rate was 2 kHz. Displacement magnitudes were estimated by applying a screen-reading cursor to the start and end points of abrupt shifts in the median-smoothed trace using MICROCAL ORIGIN version 3.5 software (see Fig. 1*B*). The 110-Hz bandwidth made an instantaneous step appear as a

The publication costs of this article were defrayed in part by page charge payment. This article must therefore be hereby marked "*advertisement*" in accordance with 18 U.S.C. §1734 solely to indicate this fact.

†To whom reprint requests should be addressed.

sloping ramp with a duration of 5–10 ms. Therefore, events having a duration of up to 15 ms were considered for scoring.

Automated Analysis. By using a raw unsmoothed positional data record, the difference between all pairs of data points separated by a time interval, τ, was calculated [$\Delta(t) = x(t) - x(t - \tau)$]. This time series was then smoothed to produce a set of values, $s(i)$, by using an iterated moving-average filter, a modified Daniell filter (15) defined as

$$s(i) = \frac{1}{w-1}\left\{\frac{1}{2}\Delta\left[i - \frac{(w-1)}{2}\right] + \sum_{j=\frac{w-1}{2}+1}^{\frac{w-1}{2}-1}\Delta[i+j] + \frac{1}{2}\Delta\left[i + \frac{(w-1)}{2}\right]\right.$$

and implemented in StatSci S+, by using a 50-point (25 ms) window, w. This procedure was repeated with multiple data records obtained under the same experimental conditions. The final histogram represents the distribution of values belonging to the set consisting of the union of the smoothed sets $s(i)$ derived from the various data records. Optimal results were obtained with $\tau \approx 60$ ms, which is comparable to the duration of kinesin's chemomechanical cycle at 20 μM ATP. Decreasing the time interval to $\tau << 60$ ms had the effect of magnifying the noise peak at the left-hand end of the distributions (data not shown), while increasing this interval to $\tau >> 60$ ms magnified the right side, i.e., peaks appearing at multiples and combinations of 3, 5, and 8 nm (data not shown). With τ fixed at 60 ms, the filtering window w could be increased to 50 ms without noticeably affecting the position of peaks; decreasing w to <25 ms compromised peak resolution (data not shown).

Controls for Analytical Artifacts. Two 400-step stochastic staircases were generated by using StatSci S+. Pause durations were exponentially distributed with a mean of 50 ms for the 8-nm stepper and 16.7 ms for the 3/5/8-nm stepper (one-third as long as for the 8-nm stepper). The sampling rate was 2 kHz. The real noise (2.6 nm, rms) was obtained from the positional record of a bead taking a 1-s pause during a run along an axoneme, with the trap stiffness set at 0.15 pN/nm and then amplified by factor of 1.52 to correct for series compliance according to Eq. **1**.

RESULTS

In our motility assays, kinesin was sparsely adsorbed onto casein-coated latex beads. The kinesin density was adjusted such that only half of the beads moved when placed in contact with an axonemal microtubule by using an optical trap. If kinesin adsorption follows Poisson statistics (7) and kinesin can reach 80 nm from its point of contact on the surface of the 1-μm bead, then >99% of the movements under these conditions can be attributed to one kinesin molecule acting alone. As the motor transported the bead against the force of an optical trap, a bright-field microscope equipped with a quadrant photodiode detector tracked the bead's position (10).

Kinesin pulled the bead along a microtubule, against a linearly increasing load, until it eventually stalled under a load of 5–6 pN, consistent with the observations of Svoboda *et al.* (9, 16). The motor could dissociate from the microtubule at any time before or during the stall, thereby ending the run. After the rapid return of the bead to the trap center, a new run would usually begin in <1 s, indicating that the kinesin was still attached to the bead. While previous studies yielded relatively few staircase-like displacement records (9, 16), the majority of our data records exhibited numerous abrupt displacement events parallel to the microtubule (Fig. 1*A*). This improved spatial resolution may be attributable to the low noise level made possible by the stiff kinesin-bead linkage in our assay (see below). The sudden displacements were best observed by adjusting the ATP concentration to 20 μM, which provided an optimal compromise between having sufficient temporal resolution between events and having a reasonable number of events in an 8-s record. To obtain a more accurate estimate of the magnitude of the displacements, the data were smoothed with a 15-ms-window sliding median filter, and the smoothed traces were then superimposed on the original traces to verify that the smoothing did not produce artifactual events. Before compiling statistics on the behavior of the bead, two selection criteria for "abrupt" displacement events were applied: (*i*) each event had to be visually distinguishable from the noise in the raw data and (*ii*) it had to occur in <15 ms (Fig. 1*B*).

To determine the behavior of the motor based on observations of bead movements, the stiffness of the kinesin-bead linkage had to be measured. In this assay, the bead behaves as though it were linked between a pair of approximately linear springs: one corresponding to the optical trap and the other to the kinesin-bead linkage [see figure 4B in Svoboda *et al.* (16)].

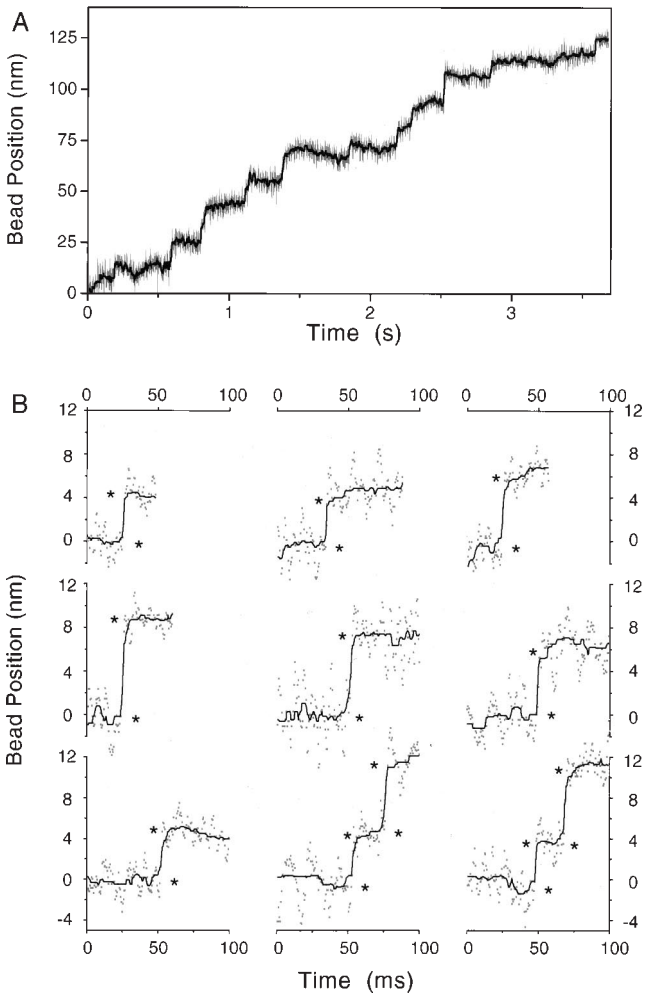

FIG. 1. (*A*) Representative stepwise displacement record for a bead being pulled away from the center of the optical trap by a single kinesin molecule. Gray line, raw data sampled at 2 kHz; black line, same data smoothed with a median filter using a 15-ms sliding window. The origin of the ordinate does not represent the center of the trap. k_{trap} = 0.019 pN/nm; [ATP] = 20 μM. (*B*) Nine examples of abrupt movements shown on an expanded scale. Shaded dots, raw data; solid lines, median-smoothed data. Asterisks are adjacent to the estimated start and end points of each discrete event. The middle and right traces in the bottom row each contain two consecutive movements of different magnitude. Occasionally, a small backward shift can be seen immediately before a movement (*Lower Right*) as reported (9). k_{trap} ranging from 0.019 to 0.150 pN/nm; [ATP] = 20 μM.

If the spring constants k_{trap} and k_{motor} are known, the time-dependent position of the motor $x_{motor}(t)$ can be calculated from that of the bead $x_{bead}(t)$, as (16)

$$x_{motor}(t) = \left(\frac{k_{motor} + k_{trap}}{k_{motor}}\right) x_{bead}(t). \quad [1]$$

(Throughout this report the reference point for the position of the motor is taken to be the point of convergence of the stalk and the two heads).

To measure k_{motor}, tension changes (10) were recorded as the kinesin-bead linkage underwent rapid 8-nm stretches and releases induced by deliberately moving the trap back and forth (Fig. 2*A*). Repeated stretch/release cycles usually proved to be free of hysteresis, and the mean linkage spring constant $\langle k_{motor} \rangle$ measured for multiple beads was 0.34 ± 0.15 pN/nm (mean ± SD; $n = 12$). This value, which agrees with other measurements

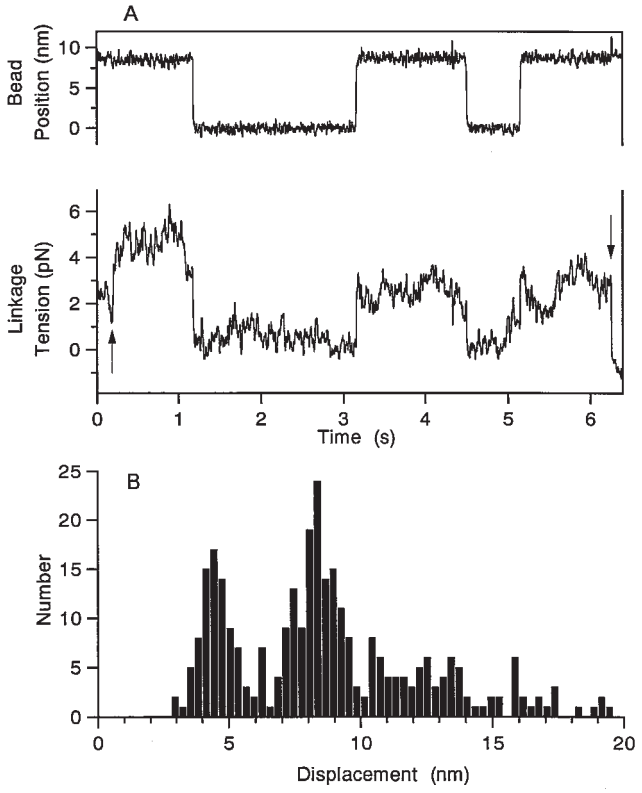

FIG. 2. Determination of the kinesin-bead linkage spring constant by rapid stretch/release experiment and distribution of abrupt motor displacements. (*A*) Optical-trap position, under calibrated feedback control, was continuously adjusted to clamp the position of the bead by countering the force exerted on it by kinesin (10). The linkage tension was derived from the magnitude of the excursion of the trap required to hold the bead in place. Upper trace, time course of bead position as the linkage is stretched and released twice by 8 nm by moving the trap while the motor is paused on the microtubule; lower trace, concomitant linkage tension. The first event in the lower trace (↑) represents a spontaneous force production by the motor, and the last event (↓) represents the dissociation of the motor from the microtubule, causing the tension to dissipate. The ratio of tension change to bead displacement averaged over multiple stretch/release cycles for several beads yielded the mean linkage spring constant $\langle k_{motor} \rangle$. The molecular nature of this linkage is poorly defined. It could involve a reversible "unpeeling" of kinesin's coiled α-helical stalk from the bead surface, a bending of the stalk, and/or longitudinal stretching. (*B*) Distribution of abrupt motor movements calculated from the distribution of abrupt bead movements ($n = 309$) from multiple beads (data not shown) by using $\langle k_{motor} \rangle = 0.34$ pN/nm in Eq. **1**. ($n = 12$ beads; $k_{trap} = 0.019$ pN/nm; [ATP] = 20 μM.) The centers of the two tall peaks were determined by double-gaussian fitting (over the range of 2.5–10.2 nm) to reside at 4.5 and 8.4 nm.

described below, is about twice as great as that reported by Meyhöfer *et al.* (17) and about 10 times greater than that reported by Svoboda *et al.* (9), possibly due to differences in bead material (1-μm latex vs. 0.6-μm silica) or assay conditions used. The linkage also usually exhibited an adequately linear behavior, as revealed by the approximate load independence of the rms noise (≤15% change in the 1- to 6-pN range).

By using $\langle k_{motor} \rangle = 0.34$ pN/nm in Eq. **1**, the distribution of abrupt bead displacements obtained from numerous different beads (data not shown) was converted into a distribution of motor displacements (Fig. 2*B*), which revealed two predominant movement sizes of 4.5 and 8.4 nm (peak positions determined by double-gaussian fitting).

To ensure that the separate peaks in this distribution were not due to different populations of beads or axonemes, the experiment was repeated by using a single bead undertaking multiple runs along the same axoneme. The distribution of abrupt bead movements was again found to contain two prominent peaks. And the positions of these peaks was found to depend on the stiffness of the optical trap, as predicted by Eq. **1**: they exhibited a leftward shift from 4.2 and 6.2 nm to 3.5 and 5.3 nm as k_{trap} was raised from 0.08 pN/nm (Fig. 3*A*) to 0.15 pN/nm (Fig. 3*B*). Fitting a function of the form $dk_{motor}/(k_{motor} + k_{trap})$, to these data, where d (the average movement of the motor) and k_{motor} are adjustable parameters, yielded a k_{motor} of 0.29 pN/nm for this particular kinesin molecule. This value is in general agreement with that obtained from the stretch/release experiments (Fig. 2*A*). The motor-displacement distributions calculated from the two bead-displacement distributions (Fig. 3 *A* and *B*) were merged into one (Fig. 3*C*), containing prominent peaks at 5.3 and 8.0 nm. These numbers are consistent with the finding of Svoboda *et al.* (9) of an 8-nm positional periodicity, but they also confirm that kinesin can undergo abrupt displacements of ≈5 nm that are smaller than the axial dimension of the tubulin dimer.

To supplement our visual estimation of movement sizes with a more objective analysis, we also used an automated method for measuring distances covered by the motor in a fixed time interval comparable to the cycle time of the motor. The most prominent peaks in the distribution were found at ≈2.6, 5.1, and 8.7 nm (Fig. 3*D*), and a few minor peaks, whose significance remains to be ascertained, were also present. The existence of peaks at ≈5 and ≈8 nm is consistent with Fig. 3*C*, while the peak at ≈3 nm was revealed only in the automated analysis. Since the repeating mechanical cycle of kinesin should conform to the 8-nm periodicity of the microtubular lattice, a 3-nm displacement might be expected to complement the abrupt 5-nm movement that was found by visual analysis. (Note that, unlike the visual method, the height of the peaks emerging from the automated analysis depends not only on the number of corresponding movements but also on the durations of the pauses preceding and following the movements).

To verify that the major peaks in the visual and automated displacement distributions were not artifactual, we analyzed computer-generated displacement traces containing instantaneous movements of 3, 5, and 8 nm or just 8 nm. These data were supplemented with real noise obtained from a kinesin-linked bead paused on an axoneme. The visual analysis method applied to the 3-, 5-, and 8-nm stepper (Fig. 3*E*) revealed a peak at ≈8 nm and poorly resolved peaks at ≈3 and ≈5 nm. The detection of the 3-nm movements in the visual analysis of the synthetic data is attributable to the fact that these movements were instantaneous, while slower movements of this magnitude, if they exist, would not be reliably resolvable from the noise in the experimental data. The automated analysis applied to the same synthetic data (Fig. 3*F*) also revealed peaks at ≈3, ≈5, and ≈8 nm in a distribution resembling the one obtained from the experimental data (Fig. 3*D*). Both analysis methods applied to the 8-nm stochastic stepper (Fig. 3 *G* and

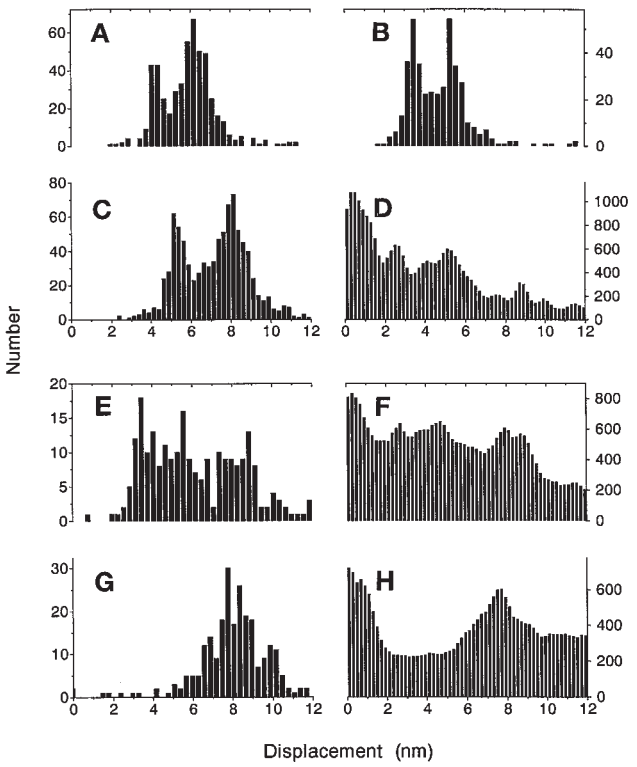

FIG. 3. Displacement magnitude distributions obtained from a single bead and controls based on synthetic data. Bead movements were measured while the trap stiffness was set at 0.08 pN/nm ($n = 515$) (*A*) and 0.15 pN/nm ($n = 402$) (*B*), demonstrating that an increase in trap stiffness causes a leftward shift of the bimodal distribution. The peak positions (obtained by double gaussian fitting) were 4.2 and 6.2 nm in *A* and 3.5 and 5.3 nm in *B*. From the magnitude of this shift, k_{motor} was calculated to be 0.29 pN/nm for this molecule. (*C*) Kinesin displacement distributions (calculated from Eq. **1**, using $k_{motor} = 0.29$ pN/nm) from *A* and *B* were merged, yielding peaks at 5.3 and 8.0 nm (determined by double gaussian fitting). (*D*) Automated determination of distances covered by a bead in 60 ms (which is comparable to the mean duration of kinesin's chemomechanical cycle at 20 μM ATP), derived from 14 motor runs. The height of each peak represents the number of 60-ms intervals during which the motor traveled a distance shown on the abscissa; these heights should not be interpreted as a direct measure of the number of abrupt displacements as in *A–C*. (*E–H*) Control analyses with computer-generated stochastic steppers. Displacement staircases were generated by using either a random mixture of 3-, 5-, and 8-nm steps (occurring with equal probability) (*E* and *F*) or just 8-nm steps (*G* and *H*). Real noise from an optically loaded bead connected to an axoneme via a paused kinesin molecule was superimposed on each staircase prior to analysis. Displacement distributions were determined by either the visual estimation method (*E* and *G*) or the automated analysis (*F* and *H*). Note the absence of peaks at either 3 or 5 nm in the distributions obtained from analyzing the 8-nm stochastic stepper (*G* and *H*). Note also that, despite the noise, 3-nm movements can be detected by the visual estimation approach if they are instantaneous (*E*).

H) produced an 8-nm peak, while no peaks were apparent at either 3 or 5 nm, thereby demonstrating that these analyses don't generate artifactual peaks at those locations. As an additional control, the automated method was applied to an unattached bead diffusing in the center of the trap, yielding a single symmetrical peak centered at zero (data not shown).

DISCUSSION

The present study has confirmed that kinesin produces abrupt movements as it travels along a microtubule and that some of these movements conform to the 8-nm periodicity of tubulin dimers along a protofilament (9). Previous studies (9, 18) reported occasional abrupt kinesin movements that were smaller than 8 nm, but the abundance of ≈5-nm movements in the present data demonstrates that such events are very common and may represent an essential component of kinesin's mechanical cycle. The results of the control analyses strongly suggest that the peak corresponding to the smaller movement is not an analytical artifact. Furthermore, at least two different bead-movement magnitudes were consistently exhibited by a single bead traveling along one axoneme, and this variability could even be seen within individual runs. Therefore, the different movement magnitudes cannot be attributed to a heterogeneity in the population of molecules.

To translate the two different bead-movement magnitudes into motor movement magnitudes (Eq. **1**), it was necessary to ascertain the spring constant of the kinesin-bead linkage. This was achieved by using two methods: (*i*) rapid stretch/release on several different molecules and (*ii*) measurement of the shift in peak positions as a function of optical trap stiffness with the same molecule. Both methods yielded a kinesin-bead linkage spring constant of ≈0.3 pN/nm. Furthermore, this elastic coupling behaved approximately linearly under loads >1 pN. Therefore, it is unlikely that the magnitude of the ≈5-nm movement of the motor was significantly miscalculated.

There could be at least two general explanations for the existence of sub-8-nm movements. Along one line of reasoning, the observed movements could reflect the lattice geometry of kinesin binding sites on the microtubule. While it is often assumed that kinesin interacts with a single protofilament as it travels along the microtubule, another interesting possibility is that the two heads interact with adjacent protofilaments. If this occurs while kinesin is straddling the microtubule's single longitudinal seam (lattice discontinuity), the motor will encounter binding sites spaced in an alternating 3- and 5-nm sequence. [Such a phenomenon could also occur along any adjacent pair of protofilaments on a type A microtubule (19, 20), but it was recently shown that the type A lattice is absent in axonemal outer doublet microtubules (21)]. Alternatively, while kinesin probably binds to only one site per tubulin dimer (22, 23), it might move with a 4-nm periodicity if it could bind consecutively to α- and β-tubulin monomers along the same protofilament. However, it is unlikely that the 5.3-nm peak in the visual analysis arose from a biased sampling of a true peak centered at 4 nm, since most of the abrupt displacements with a magnitude ≥4 nm were distinguishable from the noise.

Along a second line of reasoning, which we favor, the sub-8-nm movements might not be a direct measure of the distance between binding sites but may reveal instead that kinesin's movement from one dimer to the next along a protofilament involves at least two distinct events in the mechanical cycle. As an example, one event could be a shift to a strained forward-leaning posture arising from a large conformational change in one head, while the other event could be the jump of the partner head to a new binding site. This mechanism would impart a forward bias to the rebinding. As another example, the two events could be interpreted as the dissociation of a head from the microtubule and its forward rebinding after a measurable pause [see also related models proposed by Hackney (24)]. In either case, a single 8-nm movement would be observed whenever the two events happen to occur in rapid sequence. The notion of two sequential mechanical events per cycle is also consistent with the analysis of Svoboda *et al.* (25) of the positional variance in low-resolution displacement traces, which suggested that kinesin's cycle contains at least two rate-limiting transitions.

We are grateful to Drs. Daniel Pierce, Laura Romberg, and Karel Svoboda for helpful discussions. This work was supported by grants from the National Institutes of Health (R.D.V. and J.A.S.), the Muscular Dystrophy Association (C.M.C.), the American Heart As-

sociation (C.M.C. and R.D.V.), the Medical Scientist Training Program of Stanford University (J.T.F.), and the Human Frontiers Science Foundation (J.A.S.).

1. Hoyt, M. A. (1994) *Curr. Opin. Cell Biol.* **6,** 63–68.
2. Coy, D. L. & Howard, J. (1994) *Curr. Opin. Neurobiol.* **4,** 662–667.
3. Fujiwara, S., Kull, F. J., Sablin, E. P., Stone, D. B. & Mendelson, R. A. (1995) *Biophys. J.* **69,** 1563–1568.
4. Vale, R. D. (1993) in *Kinesin*, eds. Kreis, T. & Vale, R. (Oxford Univ. Press, Oxford), pp. 199–201.
5. Hackney, D. D. (1995) *Nature (London)* **377,** 448–450.
6. Gilbert, S. P., Webb, M. R., Brune, M. & Johnson, K. A. (1995) *Nature (London)* **373,** 671–676.
7. Block, S. M., Goldstein, L. S. & Schnapp, B. J. (1990) *Nature (London)* **348,** 348–352.
8. Howard, J., Hudspeth, A. J. & Vale, R. D. (1989) *Nature (London)* **342,** 154–158.
9. Svoboda, K., Schmidt, C. F., Schnapp, B. J. & Block, S. M. (1993) *Nature (London)* **365,** 721–727.
10. Finer, J. T., Simmons, R. M. & Spudich, J. A. (1994) *Nature (London)* **368,** 113–118.
11. Svoboda, K. & Block, S. M. (1994) *Annu. Rev. Biophys. Biomol. Struct.* **23,** 247–285.
12. Saito, K., Aoki, T., Aoki, T. & Yanagida, T. (1994) *Biophys. J.* **66,** 769–777.
13. Schnapp, B. J. & Reese, T. J. (1989) *Proc. Natl. Acad. Sci. USA* **86,** 1548–1552.
14. Gibbons, I. R. & Fronk, E. (1979) *J. Biol. Chem.* **254,** 187–196.
15. Bloomfield, P. (1976) *Fourier Analysis of Time Series: An Introduction* (Wiley, New York).
16. Svoboda, K. & Block, S. M. (1994) *Cell* **77,** 773–784.
17. Meyhöfer, E. & Howard, J. (1995) *Proc. Natl. Acad. Sci. USA* **92,** 574–578.
18. Gelles, J., Schnapp, B. J. & Sheetz, M. P. (1988) *Nature (London)* **331,** 450–453.
19. Block, S. M. & Svoboda, K. (1995) *Biophys J.* **68,** 230s–241s.
20. Howard, J. (1995) *Biophys. J.* **68,** 245s–255s.
21. Song, Y.-H. & Mandelkow, E. (1995) *J. Cell Biol.* **128,** 81–94.
22. Song, Y.-H. & Mandelkow, E. (1993) *Proc. Natl. Acad. Sci. USA* **90,** 1671–1675.
23. Harrison, B. C., Marchese-Ragona, S. P., Gilbert, S. P., Cheng, N., Steven, A. C. & Johnson, K. A. (1993) *Nature (London)* **362,** 73–75.
24. Hackney, D. D. (1994) *Proc. Natl. Acad. Sci. USA* **91,** 6865–6869.
25. Svoboda, K., Mitra, P. P. & Block, S. M. (1994) *Proc. Natl. Acad. Sci. USA* **91,** 11782–11786.